COMPDYN 2013
4th ECCOMAS Thematic Conference on
Computational Methods in Structural Dynamics and Earthquake Engineering
M. Papadrakakis, V. Papadopoulos, V. Plevris (eds.)
Kos Island, Greece, 12–14 June 2013

EXPERIMENTAL INVESTIGATION OF DYNAMIC BEHAVIOUR OF CANTILEVER RETAINING WALLS

Panos Kloukinas[1], Anna Scotto di Santolo[2], Augusto Penna[3], Subhamoy Bhattacharya[4], Matthew Dietz[4], Luiza Dihoru[4], Aldo Evangelista[2], Armando L. Simonelli[5], Colin A. Taylor[4], George Mylonakis[1,4]

[1] University of Patras
Dep. of Civil Engineering, GR-26500 Patras, GREECE
e-mail: {pkloukin, mylo}@upatras.gr

[2] University of Naples Federico II
Dep. of Hydraulics, Geotech. & Environmental Engrg, Via Claudio, 21, 82125, Naples, ITALY
e-mail: {anscotto, evangeli}@unina.it

[3] CIMA-AMRA
Via Petrile, 83054, Avellino, ITALY
e-mail: aupenna@unina.it

[4] University of Bristol
Dep. of Civil Engineering, 1-90 Queen's Building, University Walk, BS8 1TR Bristol, UK
e-mail: {s.bhattacharya, m.dietz, luiza.dihoru, colin.taylor, g.mylonakis}@bristol.ac.uk

[5] University of Sannio
Dep. of Engineering, Palazzo ex-INPS Piazza Roma, 27-1, 82100 Benevento, ITALY
e-mail: alsimone@unisannio.it

Keywords: Cantilever Retaining Walls, Earthquake Design, Dynamic Earth Pressures, Shaking Table Testing.

Abstract. *The dynamic behaviour of cantilever retaining walls under earthquake action is explored by means of 1-g shaking table testing, carried out on scaled models at the Bristol Laboratory for Advanced Dynamics Engineering (BLADE), University of Bristol, UK. The experimental program encompasses different combinations of retaining wall geometries, soil configurations and input ground motions. The response analysis of the systems at hand aimed at shedding light onto the salient features of the problem, such as: (1) the magnitude of the soil thrust and its point of application; (2) the relative sliding as opposed to rocking of the wal land the corresponding failure mode; (3) the importance/interplay between soil stiffness, wall dimensions, and excitation characteristics, as affecting the above. The results of the experimental investigations are in good agreement with the theoretical models used for the analysis and are expected to be useful for the better understanding and the optimization of earthquake design of this type of retaining structure.*

1 INTRODUCTION

Reinforced concrete cantilever retaining walls represent a popular type of retaining system. It is widely considered as advantageous over conventional gravity walls as it combines economy and ease in construction and installation. The concept is deemed particularly rational, as it exploits the stabilizing action of the soil weight over the footing slab against both sliding and overturning, thus allowing construction of walls of considerable height.

The traditional approach for the analysis of cantilever walls is based on the well-known limit equilibrium analysis, in conjunction with a conceptual vertical surface AD (Fig. 1b,c) passing through the innermost point of the wall base (vertical virtual back approach). A contradictory issue in the literature relates to the calculation of active thrust acting on the virtual wall back, under a certain mobilized obliquity ranging naturally from 0 (a perfectly smooth plane) to φ (a perfectly rough plane). Efforts have been made by different investigators to establish the proper roughness for the analysis and design or this type of structures under static loading [1, 2]. Nevertheless, the issue of seismic behaviour remains little explored. Modern Codes including Eurocode [3] and the Italian Building Code [4], do not explicitly refer to cantilever walls. The current Greek Seismic Code [5] addresses the case of cantilever retaining walls by adopting the virtual back approach in the context of a pseudo-static analysis under the assumption of gravitational Rankine conditions [6] and various geometric constraints.

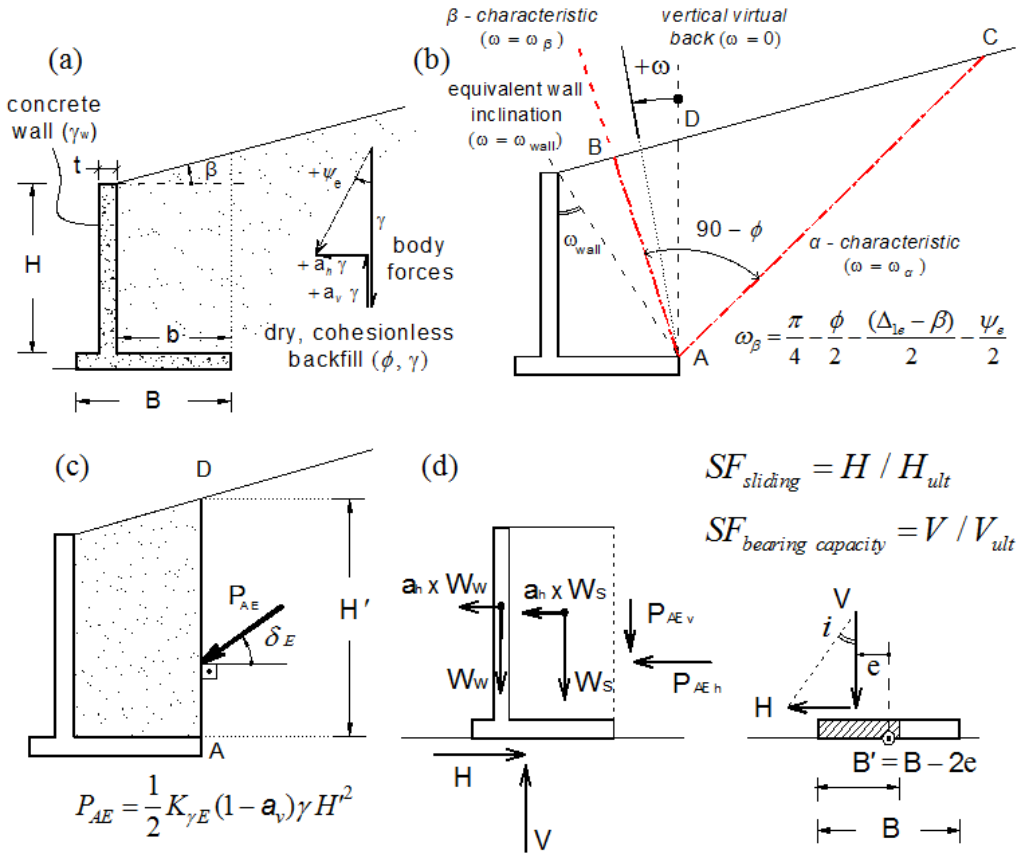

Figure 1: Pseudo-dynamic analysis of cantilever retaining walls for seismic loading: (a) Problem under consideration, (b) seismic Rankine stress field characteristics, (c) Modified virtual back approach by stress limit analysis, (d) Stability analysis of wall foundation according to Meyerhof (EC 7).

Recent theoretical findings obtained by means of stress limit analysis [1, 2, 7] for the seismic problem of Fig. 1a indicate that a uniform Rankine stress field develops in the backfill,

when the wall heel is sufficiently long and the stress characteristics do not intersect the stem of the wall ($\omega_\beta < \omega_{wall}$). Given that the stress characteristics inclination depends on acceleration, Rankine condition is valid for the vast majority of cantilever walls under strong seismic action. This is applicable even to short heel walls, with an error of about 5% [8, 9].

Following the aforementioned stress limit analysis studies, closed-form expressions are available for the pseudo-dynamic earth pressure coefficient K_{AE} and the resultant thrust inclination, δ_E (Fig.1c), given by [2]:

$$\delta_E = \tan^{-1}\left[\frac{\sin\varphi \sin\left(\Delta_{1e} - \beta + \psi_e\right)}{1 - \sin\varphi \cos\left(\Delta_{1e} - \beta + \psi_e\right)}\right] \quad (1)$$

where $\Delta_{1e} = \sin^{-1}[\sin(\beta+\psi_e)/\sin\varphi]$ and $\psi_e = \tan^{-1}[a_h/(1-a_v)]$ are the so-called Caquot angle and the inclination of the overall body force in the backfill. The same result for δ_E has been derived, in a somewhat different form, by Evangelista et al. [1]. In the case of gravitational loading ($\psi_e = 0$), the inclination δ_E equals the slope angle β, coinciding to the classical Rankine analysis. In presence of a horizontal seismic component ($\psi_e > 0$), δ_E is always greater than β, increasing with ψ_e up to the maximum value of φ, improving wall stability. The robustness of the above analysis becomes evident since under a mobilized inclination δ_E, the stress limit analysis and the Mononobe-Okabe formula results coincide. These findings have been confirmed by numerical investigations [1, 7].

A second key issue relates to the stability analysis shown in Figure 1c. Traditionally, stability control of retaining walls is based on safety factors against bearing capacity, sliding and overturning. Of these, only the first two are known to be rationally defined, whereas safety against overturning is known to be misleading, lacking a physical basis [2, 4, 10, 11]. It is important to note that the total gravitational and seismic actions on the retaining wall are resisted upon the external reactions H and V acting on the foundation slab. The combination of these actions together with the resulting eccentricity e, determines the bearing capacity of the wall foundation based on classical limit analysis procedures for a strip footing subjected to an eccentric inclined load (e.g. EC7, EC8). This suggests that the issue of wall stability is actually a footing problem and from this point of view, understanding the role of the soil mass above the foundation slab and the soil-wall interaction is of paramount importance. The above observations provided the initial motivation for the herein-reported work.

2 SHAKING TABLE EXPERIMENTAL INVESTIGATION

The dynamic behaviour of L-shaped cantilever walls was explored by means of 1-g shaking table testing. The aim of the experimental investigation is to provide a better understanding of the soil-wall dynamic interaction problem, the relationship between design parameters, stability safety factors and failure mechanisms, and the validation of the seismic Rankine theoretical model. The test series were conducted to the Bristol Laboratory for Advanced Dynamics Engineering (BLADE), University of Bristol, UK. Details on the experimental hardware, materials, configurations and procedure are provided in the ensuing.

2.1 Experimental hardware

Earthquake Simulator (ES)

The 6DOF ES consists of a 3 m x 3 m cast aluminium platform weighing 3.8 tonnes, with payload capacity of 15 tonnes maximum and operating frequency range of 1-100Hz. The platform sits inside an isolated, reinforced concrete seismic block that has a mass of 300

tonnes and is attached to it by eight 70 kN servo hydraulic actuators of 0.3m stroke length. Hydraulic power for the ES is provided by a set of 6 shared variable volume hydraulic pumps providing up to *900 litres/min* at a working pressure of *205 bar,* with maximum flow capacity of around *1200 litres/min* for up to 16 seconds at times of peak demand with the addition of extra hydraulic accumulators.

Equivalent Shear Beam (ESB) Container

The apparatus, shown in Figure 2a, consists of eleven rectangular aluminium rings, which are stacked alternately with rubber sections to create a flexible box of inner dimensions 4.80m long by 1m wide and 1.15m deep [12]. The rings are constructed from aluminium box section to minimize inertia while providing sufficient constraint for the K_0 condition. The stack is secured to the shaking table by its base and shaken horizontally lengthways (in the x direction). Its floor is roughened by sand-grain adhesion to aid the transmission of shear waves; the internal end walls are similarly treated to enable complementary shear stresses. Internal side walls were lubricated with silicon grease and covered with latex membrane to ensure plane strain conditions.

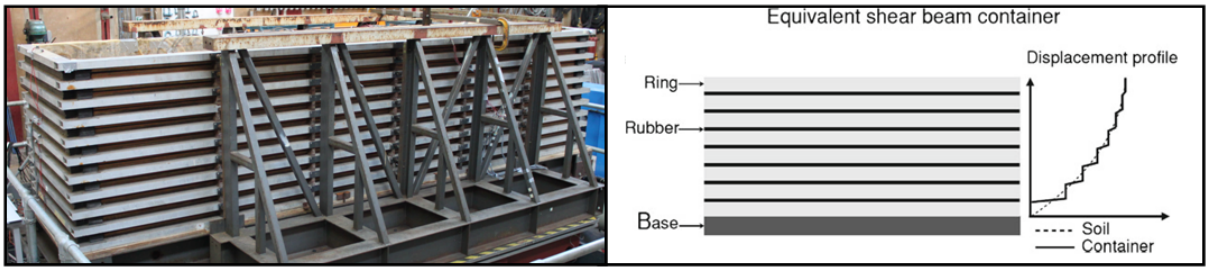

(a) **(b)**

Figure 2: Equivalent shear beam container ("shear stack")

This type of containers should be ideally designed to match the shear stiffness of the soil contained in it, as depicted in Figure 2b. However, the shear stiffness of the soil varies during shaking depending on the strain level. Therefore, matching of two stiffnesses (end-wall and the soil) is possible only at a particular strain level. The "shear stack" at the University of Bristol is designed considering a level of strain in the soil close to failure (0.01–1%). Therefore, the box is much more flexible than the contained soil and, as a consequence, the soil will always dictate the overall behaviour of the container [13]. Indeed the resonant frequency and damping of the container in the first shear mode in the long direction when empty were measured prior to testing at 5.7Hz and 27% respectively, which is sufficiently different from the soil material properties.

Instrumentation

As seen in Figure 3, 21 1-D accelerometers have been used to monitor the shaking table, the shear stack and the wall-soil system, with the main area of interest laying on the wall itself and the soil mass in its vicinity, as well as the response of the free field. 4 LVDT transducers were employed to measure the dynamic response and permanent displacements of the wall and 32 strain gauges were attached on the stem and the base of the wall, on three cross sections, to monitor the bending of the wall. The signal conditioning was made via appropriate amplifier and filter modules and data acquisitions frequency was set at 1024 Hz. Additionally to the 57 data channels employed overall, a grid of colored sand was used for monitoring the settlement of the backfill surface.

2.2 Shaking table model setup

Model geometry

The dimensions of the model are illustrated in Figure 3, with the type and the positions of the instrumentation used. The model consists of an L-shaped retaining wall supporting a backfill of thickness 0.6m and length 5 times its thickness, resting on a 0.4m thick base soil layer (equal to the wall foundation width, B). The properties of the soil layers and detailed description of the instrumentation and the various wall configurations are provided in below.

The retaining wall was constructed from Aluminium 5083 plates of 32mm thickness. The width of the wall stem is 970mm. A central wall segment of 600mm width was created by two 1mm thick vertical slits penetrating 400mm down into the wall. The location of the slits were 185mm from each side of the wall stem. The base of the wall is subdivided into four 240mm-wide aluminium segments that are each secured to the wall stem using three M12 bolts. Properties of the aluminium alloy are: unit weight γ = 27 kN/m^3, Young's modulus E = 70GPa, Poisson's ratio ν = 0.3.

Soil material properties

The required soil configuration consists of a dense supporting layer and a medium dense backfill. The material proposed for both layers is Leighton Buzzard (LB) sand BS 881-131, Fraction B (D_{50} *=0.82 mm,* G_s*=2.64 Mg/m*^{3}*,* e_{min} *= 0.486,* e_{max} *= 0.78)*. This particular soil has been extensively used in experimental research at Bristol and a wide set of strength and stiffness data is available (detailed references in [13]). The empirical correlation between peak friction angle φ and relative density D_r provided by the experimental work of Cavallaro et al. [14] was used for a preliminary estimation of the soil strength properties.

The packing density for each layer was determined from sand mass and volume measurements during the deposition; corresponding predictions for peak friction angles are summarized in Table 1. The base deposit was formed by pouring sand in layers of *150-200 mm* from a deposition height of 0.6m, and then densifying it by shaking. After densification the height of the layer was reduced to 390mm. The top layer was formed by pouring sand in axisymmetric conditions close to the centre of the desired backfill region, without any further densification. The pouring was carried out by keeping the fall height steady, approximately equal to 200mm, in order to minimize the densification effect of the downward stream of sand.

Model wall configurations

Three different Configurations (#1, #2, #3) for the wall model presented in Fig. 3 were used to provide different response in sliding and rocking of the base. The characteristics of these configurations are shown in Table 2. After testing Configuration 1, the wall model was modified for Configuration 2. The wall heel was shortened by 50mm and the toe was totally removed. In Configuration 3, the geometry of Configuration 2 was retained, after increasing the frictional resistance of the base interface from 23.5^o to 28^o (approximately equal to the critical state angle), by pasting rough sandpaper. The interface friction angles were measured in-situ by means of static pull tests on the wall. The differences between these three Configurations in terms of a pseudo-dynamic stability analysis according to EC7 are summarised in Table 2, ranging from a purely sliding-sensitive wall (Configuration 1), to a purely rotationally sensitive one (Configuration 3).

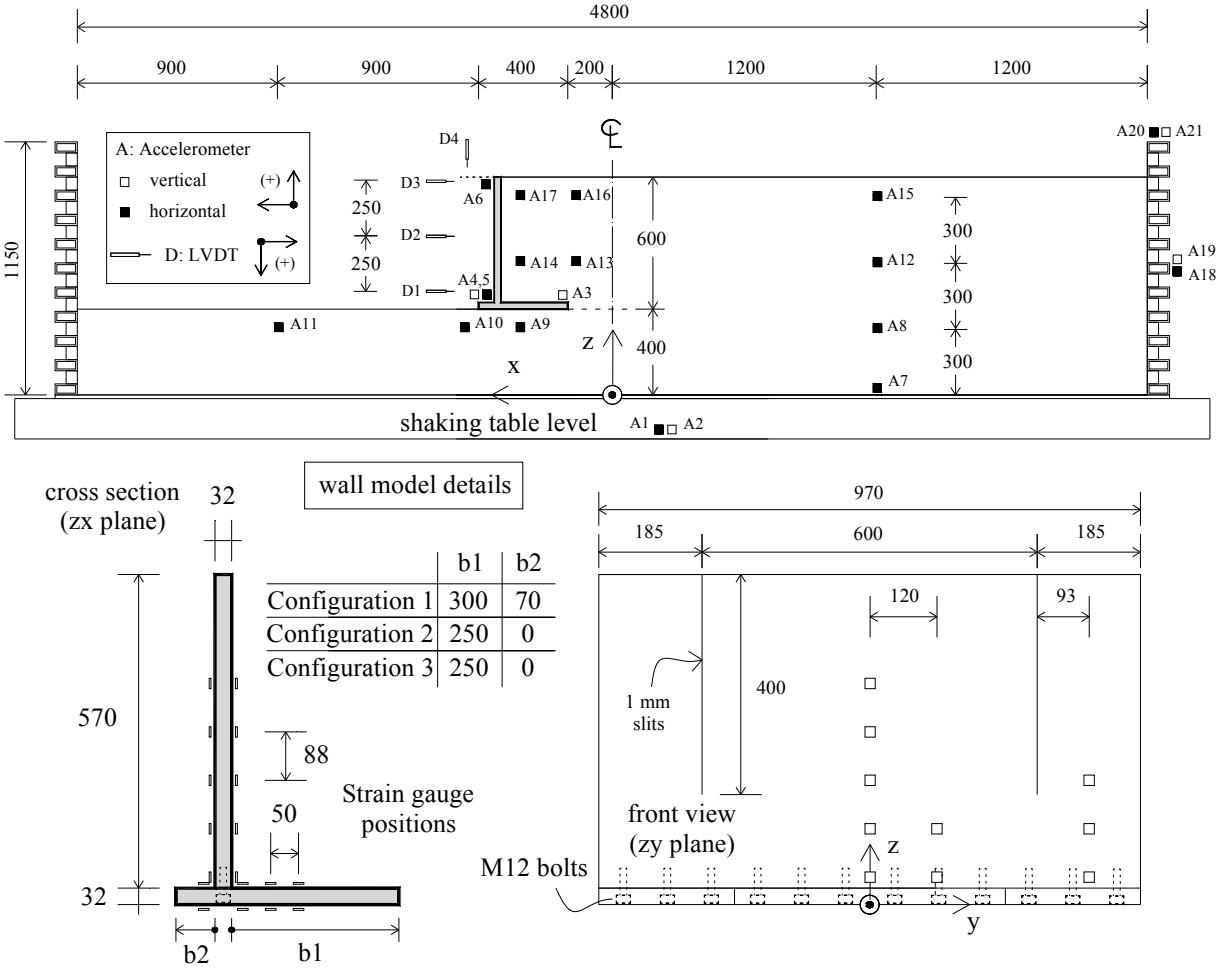

Figure 3: Illustration of geometry and instrumentation of the shaking table model (dimensions in mm)

Soil layers	Thickness (mm)	Voids ratio, e	Relative density, D_r (%)	Unit weight (kN/m^3)	Friction angle, φ(°) Cavallaro et al. (2001)
Foundation	390	0.61	60	16.14	42
Backfill	600	0.72	22	15.07	34

Table 1: Soil properties

Test configuration	Critical acceleration for $SF_{sliding} = 1$	$SF_{Bearing\ capacity}$ at critical sliding acceleration	Critical acceleration for $SF_{Bearing\ capacity} = 1$	$SF_{sliding}$ at critical bearing capacity acceleration
Configuration 1	0.18g	7.45	0.35g	0.68
Configuration 2	0.14g	1.46	0.17g	0.93
Configuration 3	0.23g	0.44	0.17g	1.14

Table 2: Pseudostatic critical accelerations and associated safety factors (SF)

2.3 Experimental procedure

Each model Configuration was tested under the same dynamic excitation, described in detail in the following paragraphs. Two different input motions, harmonic and earthquake, were used in the form of sequential, increasing amplitude time histories. The dynamic properties of the soil layers and the soil-wall interactive system were investigated by means of the white noise exploratory procedure described below. This kind of testing was repeated after every severe yielding of the system to track for significant chances in the dynamic properties.

White noise excitation

During white noise exploratory testing, a random noise signal of bandwidth *1-100 Hz* and *RMS* acceleration = 0.005g was employed. During each exploratory series test, and simultaneous data acquisition, system transmissibility was monitored using a two-channel spectrum analyser. The analyser computes the frequency response function (FRF) between the input and the output signals of interest. Natural frequency and damping values for any resonances up to 40Hz (i.e. within the seismic frequency range) were determined for well-defined resonances using the output of the analyser's curve fitting algorithm by means of a least-squares error technique. Additionally, transfer functions can be determined between any pair of data channels to get a clear view of the system dynamics.

Harmonic excitation

This type of input acceleration was imposed by sinusoidal excitation consisting of 15 steady cycles. To smoothen out the transition between transient and steady-state response, the excitation comprises of a 5-cycle ramp up to full test level at the beginning of the excitation, and a 5-cycle ramp down to zero at the end. With reference to frequency and acceleration level, a set of 5 frequencies (4, 7, 13, 25 and 43 Hz) was used at low acceleration amplitude of 0.05g, to study the dynamic response of the system. The excitation frequency of 7Hz was then selected for a series of harmonic excitations with increasing amplitude, until failure. The conditions of the excitation are considered to be essentially pseudostatic, as the above frequency is much smaller than the resonant frequencies of the system, with respect to both the free field and the soil-wall system.

Earthquake excitation

Three earthquake records from the Italian and American database were selected for the earthquake testing. Specifically, the Tolmezzo record from the Friuli, 1976 earthquake, the Sturno record from Irpinia, 1980 and the Northridge record from Los Angeles, 1994. The authentic signals were scaled by a frequency scale factor of 5, derived from the scaling law $n^{0.75}$, which is valid for 1-g modelling [15], assuming a geometrical scale factor n = 9, corresponding to a prototype of 5.4m high. The frequency-scaled signals were applied at low acceleration amplitude of 0.05g to measure the dynamic response of the model and then the Sturno record was selected for carrying out increasing amplitude dynamic testing, until failure in sliding or rocking of the retaining wall.

3 EXPERIMENTAL RESULTS AND DISCUSSION

Some characteristic experimental measurements are presented in Figures 4 to 8, relative to failure mechanisms, accelerations, dynamic and permanent displacements and bending moments, organized in sets of graphs suitable for direct comparisons. Most of the results presented herein mainly relate to Configurations 1 and 3, for they exhibit yielding near similar acceleration conditions but in different modes. Limited results are presented for Configuration 2, which is significantly weaker compared to the others, failing almost simultaneously in

foundation sliding and rotation (i.e., bearing capacity) mode, thus is less important for comparison reasons.

In Figure 4, measured settlement profiles at the state of failure are plotted together with the assumed failure mechanisms for Configurations 2 and 3. The following are worthy of note: *First,* these failure mechanisms were observed only for transient earthquake loading, whereas in the case of harmonic excitation, the settlement profile could not clearly reveal the emergence of the main failure planes, as it had more-or-less a smooth parabolic shape. This can be explained in view of a non-uniform settlement and deformation mechanism and stronger dynamic effects imposed by earthquake loading. Although there is actually not a "rigid block" response in the retained soil mass, the experimental findings show that the earthquake excitation induces a more uniform acceleration distribution within the retained soil material, which corresponds to a more uniform stress field, as assumed in the pseudo-static analyses. *Second,* the assumed failure mechanisms confirm the estimations based on the material properties, the stability analysis and the yield accelerations presented in Tables 1 and 2 respectively.

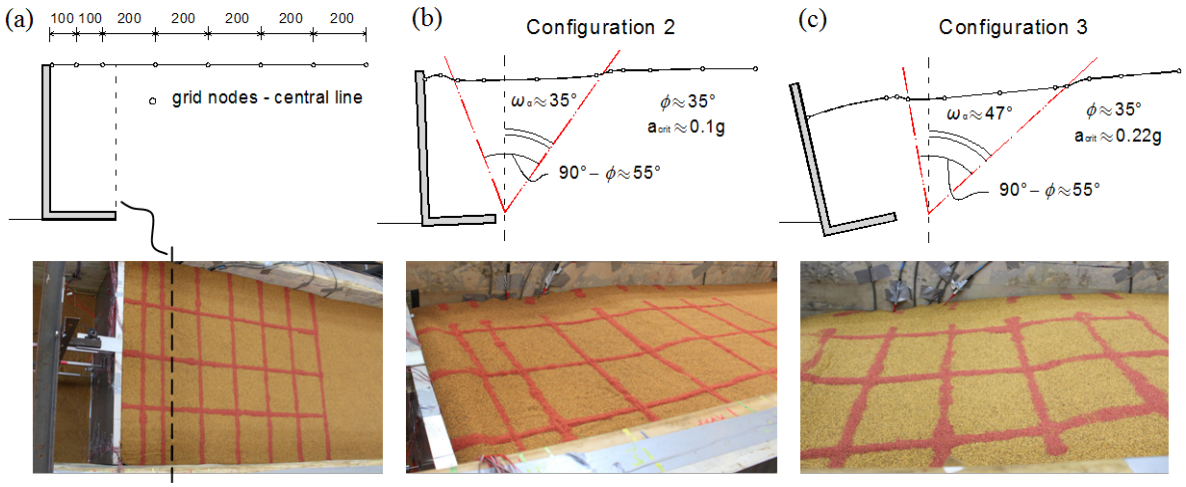

Figure 4: Backfill surface settlement distribution at failure: (a) initial grid geometry - dimensions in mm, (b),(c) settlement distributions for Configurations 2 and 3, respectively.

The measurements of system displacement for all tested configurations are summarized in Figure 5. The total, cumulative settlement and rotation of the wall, for each series of sequential input motions are presented in Figures 5a and 5b, and the incremental displacements for each input motion are presented in Figures 5c-5e, indicating different behaviour of the wall models under the same input. The measurements confirm the predictions for the expected failure modes and the levels of critical acceleration. The sliding failure is clearly visible in Configuration 1, as is the bearing capacity failure in Configuration 3. Configuration 2 although designed to be weaker in sliding, also exhibits significant rotational deformations caused by the high eccentricities induced by the seismic thrust. Rotational deformations are also observed in Configuration 1 for high acceleration levels, revealing that walls resting on a compliant base exhibits local bearing capacity failure near the toe, due to high compressive stress concentration. This observation elucidates the importance of properly designing retaining structures to avoid development of significant rotational response.

Results from Configurations 1 and 3 under harmonic excitation are plotted together in Figure 6. The following can be observed: *First* the response of each Configuration is as

expected. A translational response mode is evident in Configuration 1 and a rocking one in Configuration 3, respectively. Sliding discontinuities are obvious on the acceleration time histories of Configuration 1 (Fig 6a), at a critical acceleration slightly higher than that of Table 2. Note that the translational yield acceleration is not steady, but always increases after every successive yielding, as even a small rotation causes penetration of the wall toe into the foundation soil thus increasing passive resistance. On the other hand, Configuration 3 starts rotating at initiation of yielding, without any evidence of sliding discontinuities on the recorded accelerogram. *Second*, in both cases the wall stem appears to have an amplified response, mainly because of foundation rocking and secondarily of pure bending of the stem. Naturally, this is more evident in Configuration 3. *Third*, both models exhibit a consistent, repeatable, behaviour with respect to yielding.

The same results for earthquake loading on Configurations 1 and 3 are presented in Figure 7. In this case, the input motion contains higher effective peak accelerations, but the number of important strong cycles (half cycle pulses) is only three. A sliding failure pattern is, again, clearly visible in Configuration 1. Likewise, a bearing capacity failure in Configuration 3 is apparent, due to high eccentricities induced by seismic thrust. An important notice about the failure modes arising from the combination of the two comparisons is that the bearing capacity failure is more affected by the input acceleration level, whereas the behaviour of pure sliding mechanisms is mainly controlled by the time interval of the strong motion, as established from sliding block theory. Accordingly, rotational mechanisms appear to be more critical under strong earthquakes, even though they are strong enough against sliding (Fig 6d and Fig 7d). Moreover, some rotational deformation is also observed in Configuration 1 for high acceleration level, revealing that any wall resting on a compliant base exhibits local bearing capacity failure near the toe, due to concentration of high compressive stresses. This observation elucidates the importance of properly designing retaining structures to avoid development of significant rotational response.

From the acceleration distributions of Figs 6c and 7c, it is evident that the earthquake loading results to conditions which are closer to the assumptions of pseudostatic analysis, as a soil mass moving together with the wall is evident, especially for the rotational mode of Configuration 3. Contrary to earthquake excitation, under harmonic loading wall and soil appear to respond in a quite different way.

Peak seismic increments of bending moments are compared in Figs 6e and 7e. A noteworthy observation is that the earth pressure on the wall increases when the system moves towards the backfill, that is for an acceleration not critical for overall stability. On the other hand, at yielding acceleration of the system, earth pressure on the stem is minimum. This is in agreement with the findings of other recent experimental and numerical studies [16, 17]. Comparing Configurations 1 and 3, it can be clearly identified that rotational modes induce lower earth pressure on the wall, but different distribution leading to a higher point of application of the thrust.

Finally, the response of Configuration 2 to harmonic and earthquake excitation with PGA = 0.17g presented in Fig. 8, exhibits a similar behaviour to both Configurations 1 and 3, resulting to simultaneous sliding and rotational failure. As seen from both the acceleration time histories (Fig. 8a) and the failure mechanisms (Fig. 8b) the sliding failure mode prevails, which is consistent to the critical accelerations estimated in Table 2.

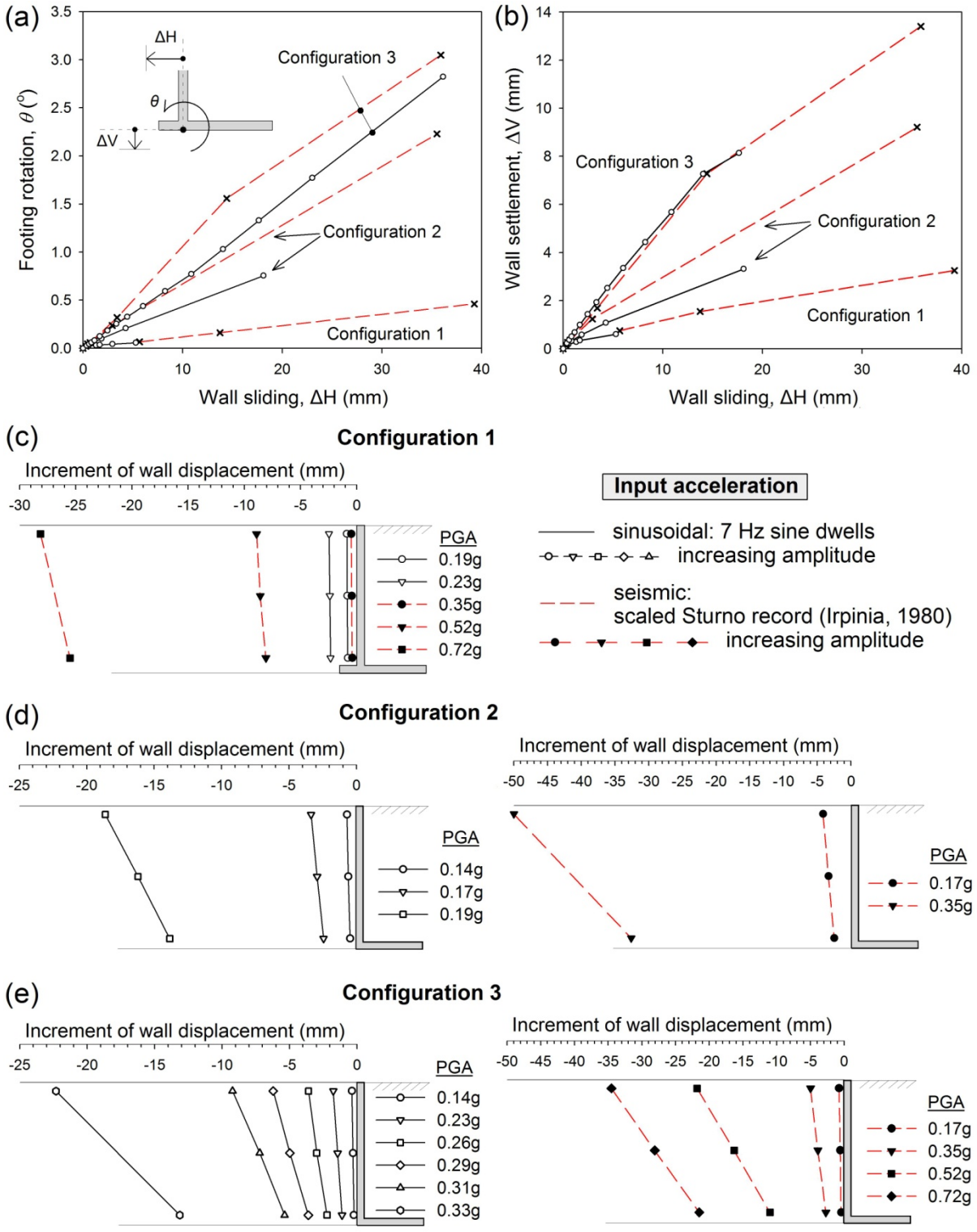

Figure 5: Measurements of wall displacement and rotation for all configurations and various base excitations. (a) Cumulative footing rotation versus sliding (LVDT-D1), (b) Cumulative footing settlement (LVDT-D4) versus sliding, (c), (d) and (e) Incremental wall displacement (LVDTs D1-D2-D3) for configurations 1, 2 and 3, respectively

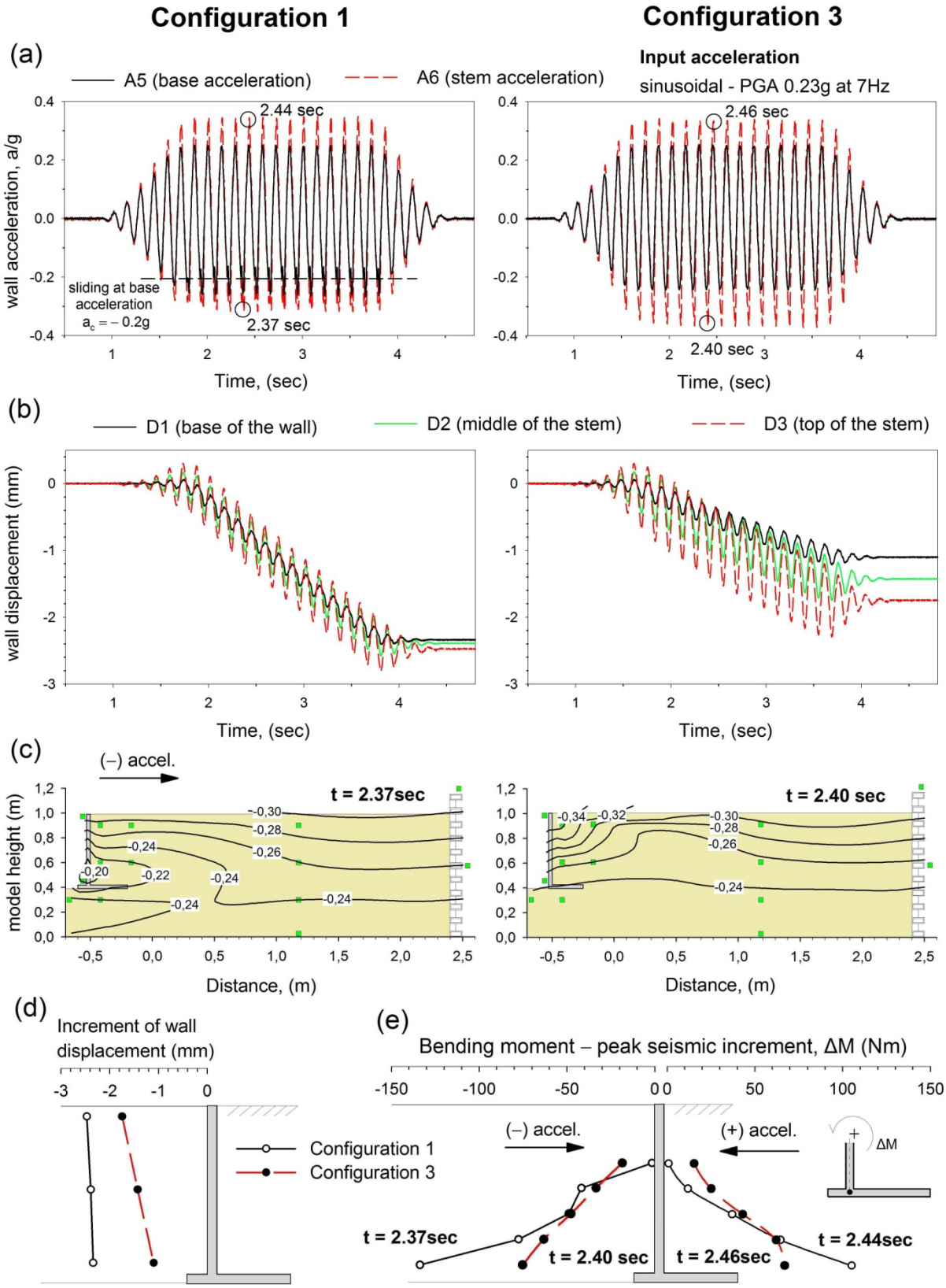

Figure 6: Comparison of typical experimental results for Configurations 1 and 3 under harmonic-sinusoidal excitation: (a) measured wall accelerations, (b) corresponding wall displacements, (c) negative acceleration distribution (maximum inertial forces towards the wall), (d) increment of wall displacement (LVDTs D1-D2-D3) and (e) peak seismic increment of bending moment for positive and negative acceleration.

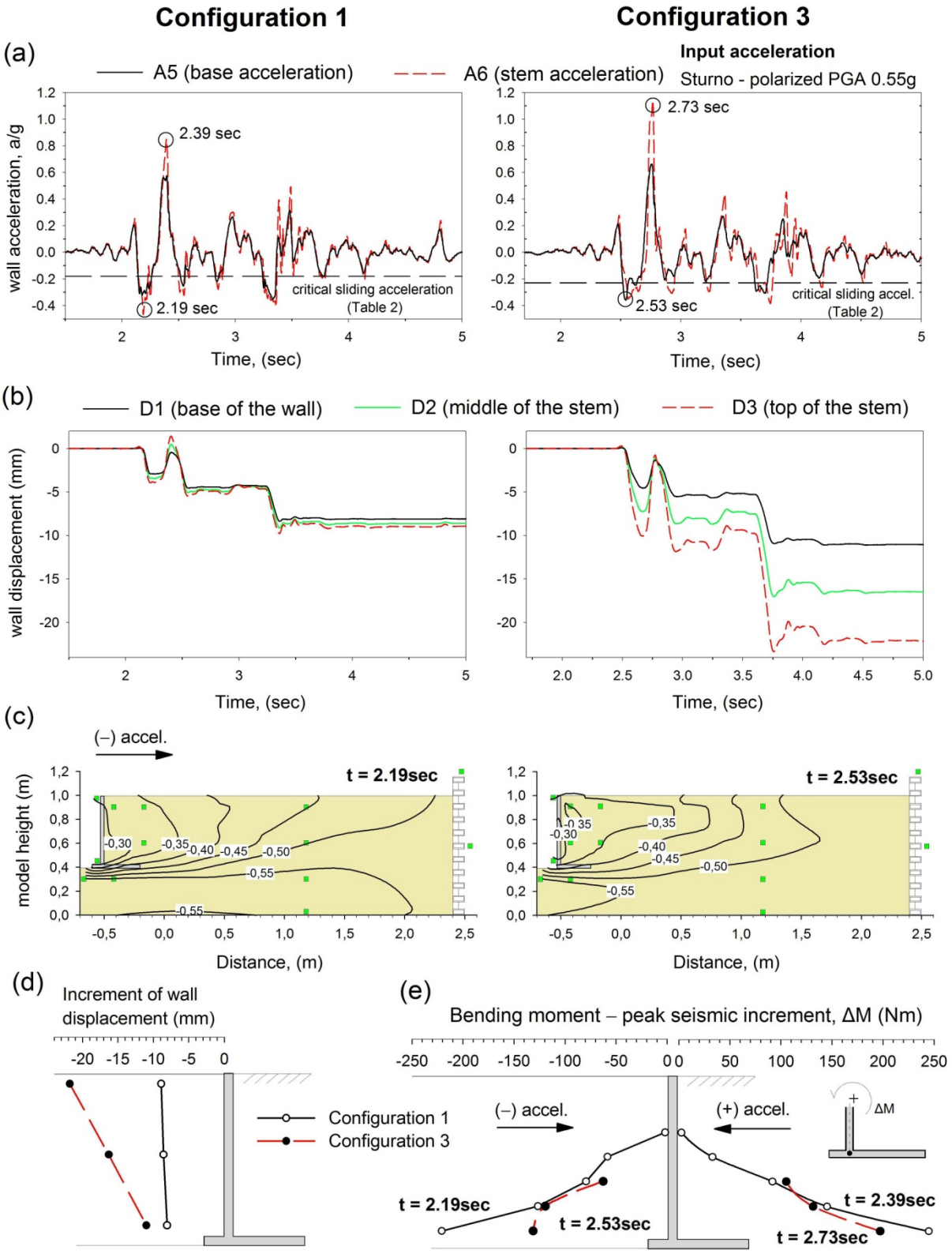

Figure 7: Comparison of typical experimental results for Configurations 1 and 3 under seismic excitation: (a) measured wall accelerations, (b) corresponding wall displacements, (c) negative acceleration distribution (maximum inertial forces towards the wall), (d) increment of wall displacement (LVDTs D1-D2-D3) and (e) peak seismic increment of bending moment for positive and negative acceleration.

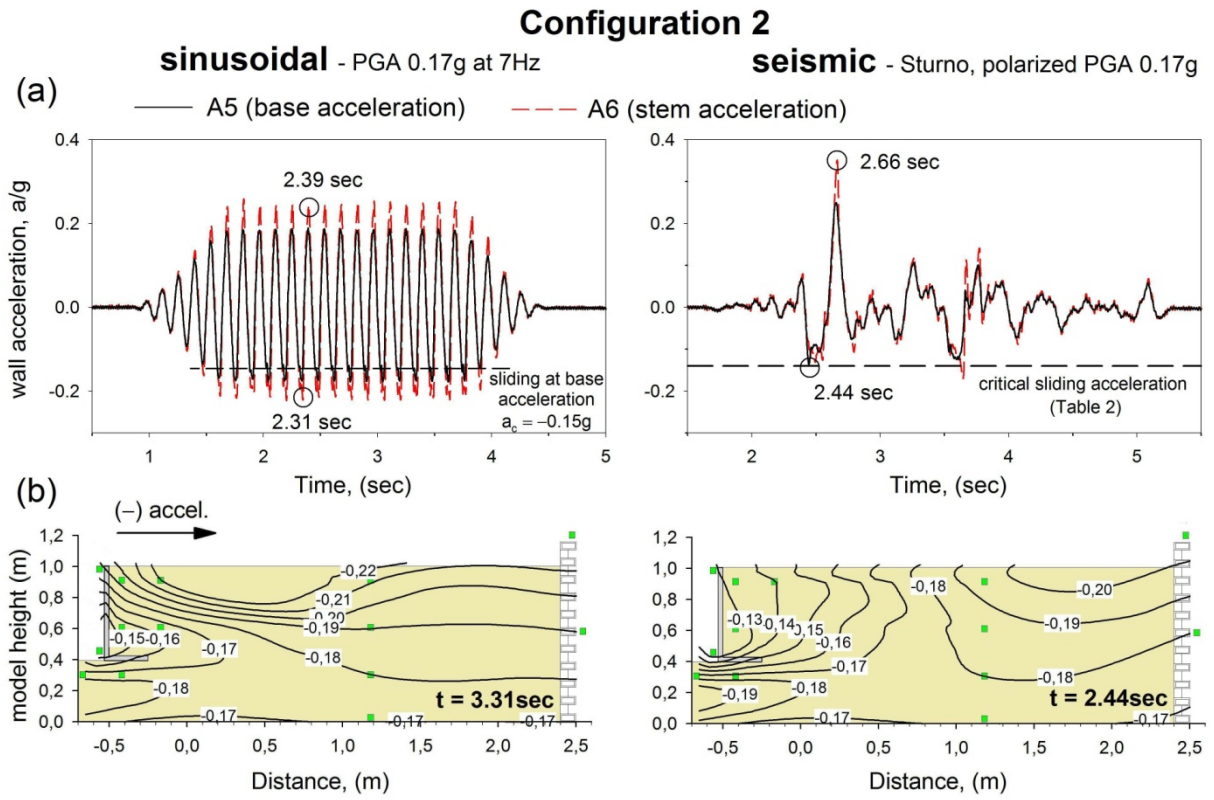

Figure 8: Typical experimental results for Configuration 2: (a) measured wall accelerations for harmonic sinusoidal and seismic excitation, (b) negative acceleration distribution (maximum inertial forces towards the wall)

4 CONCLUSIONS

A series of shaking table tests on scaled models of cantilever retaining walls were conducted in BLADE laboratory at University of Bristol. The initial motivation of this experimental study was the validation of recent stress limit analysis solutions for the seismic design of this type of retaining structures [1, 2] in conjunction with the absence of any specific, relative regulations in established seismic codes, including the EC-8. Special issues related to stability design and response of walls founded on a compliant base were also addressed. Preliminary interpretation of the experimental findings confirms the predictions of the theoretical analysis with reference to the failure mechanisms and the critical yield accelerations of the system. Pseudo-static stability analysis proves to behave adequately for both harmonic and seismic excitation, although important dynamic effects are evident in the first case, dealing with the response of the backfill and the wall stem. On the other hand, earthquake loading results to conditions which are closer to the assumptions of the pseudo-static analysis, namely the uniform distribution of the acceleration and the "rigid block" response of the backfill. Finally, the responses of the various wall configurations confirm the "equivalent footing" interpretation of wall stability and highlight the importance of a proper design of walls founded on compliant base against sliding and rocking.

ACKNOWLEDGEMENT

The research leading to these results has received funding from the European Union Seventh Framework Programme (FP7/2007-2013) under grant agreement n° 227887, SERIES.

REFERENCES

[1] Evangelista A., Scotto di Santolo A., Simonelli A.L., Evaluation of pseudostatic active earth pressure coefficient of cantilever retaining walls. *Soil Dynamics & Earthquake Engineering*, **30:11**, 1119-1128, 2010

[2] Kloukinas, P. and Mylonakis, G., Rankine Solution for seismic earth pressures on L-shaped retaining walls. *5 ICEGE*, Santiago, Chile, January 10-13, 2011

[3] Eurocode 8, *Design provisions for earthquake resistance of structures, Part 5*. CEN E.C. for Standardization, Bruxelles, 2003

[4] NTC, *Italian Building Code*. DM 14 Jan., G.U. n. 29, 4 Feb., n. 30, 2008

[5] EAK 2000, *Greek Seismic Code*. Earthquake Planning and Protection Organization, Athens, 2003

[6] Rankine, W.J.M, On the stability of loose earth. *Phil. Trans. of the Royal Soc. of London*, **147,** 9 – 27, 1857

[7] Evangelista A., Scotto di Santolo A., Dynamic active earth pressure on cantilever retaining walls. *Computers and Geotechnics*, **38:8**, 1041-1051, 2011

[8] Huntington W, *Earth pressures and retaining walls*. New York: John Wiley, 1957

[9] Greco VR., Active earth thrust on cantilever walls with short heel. *Canadian Geotechnical Journal*, **38:2**, 401–409, 2001

[10] Greco, V.R., Stability of Retaining Walls Against Overturning. *Journal of Geotechnical & Geoenviromental Engineering*, ASCE, **123:8**, 778 – 780, 1997

[11] Eurocode 7, *Geotechnical Design.* CEN, E.C. for Standardization, Bruxelles, 2003

[12] Crewe AJ, Lings ML, Taylor CA, Yeung AK, Andrighetto R, *Development of a large flexible shear stack for testing dry sand and simple direct foundations on a shaking table*. In: Elnashai (ed) European seismic design practice, Balkema, Rotterdam, 1995

[13] Bhattacharya S., Lombardi D., Dihoru L., Dietz M. S., Crewe A.J., and Taylor. C.A, *Chapter 8: Model Container Design for Soil-Structure Interaction Studies*", in M.N. Fardis and Z.T. Rakicevic (eds.) Role of Seismic Testing Facilities in Performance-Based Earthquake Engineering SERIES Workshop, Geotechnical, Geological and Earthquake Engineering 22, Springer Science+Business Media B.V, 2012

[14] Cavallaro A, Maugeri M, Mazzarella R., Static and dynamic properties of Leighton Buzzard sand from laboratory tests. *Proc. of 4th int. conf. on recent adv. in geotech. earthquake engrg. and soil dyn. and symposium in honour of Prof. WD Liam Finn*, San Diego, California, March 26–31, 2001

[15] Muir Wood D., Crewe A. & Taylor C.A., Shaking Table Testing of Geotechnical Models. *International Journal of Physical Modelling in Geotechnics*, **2**, 01-13, 2002

[16] Green R.A and Olgun CG., Response and Modeling of Cantilever Retaining Walls Subjected to Seismic Motions. *Computer-Aided Civil and Infrastructure Engineering* **23:4**, 309–322, 2008

[17] Al Atik L., Sitar N., Seismic Earth Pressures on Cantilever Retaining Structures, *Journal of Geotechnical and Geoenvironmental Engineering*, ASCE, **136:10**, 1324-1333, 2010